OVERLAPPING SCHWARZ ALGORITHMS FOR ALMOST INCOMPRESSIBLE LINEAR ELASTICITY

MINGCHAO CAI *, LUCA F. PAVARINO †, AND OLOF B. WIDLUND ‡

Abstract. Low order finite element discretizations of the linear elasticity system suffer increasingly from locking effects and ill-conditioning, when the material approaches the incompressible limit, if only the displacement variable are used. Mixed finite elements using both displacement and pressure variables provide a well-known remedy, but they yield larger and indefinite discrete systems for which the design of scalable and efficient iterative solvers is challenging. Two-level overlapping Schwarz preconditioner for the almost incompressible system of linear elasticity, discretized by mixed finite elements with discontinuous pressures, are constructed and analyzed. The preconditioned systems are accelerated either by a GMRES (generalized minimum residual) method applied to the resulting discrete saddle point problem or by a PCG (preconditioned conjugate gradient) method applied to a positive definite, although extremely ill-conditioned, reformulation of the problem obtained by eliminating all pressure variables on the element level. A novel theoretical analysis of the algorithm for the positive definite reformulation is given by extending some earlier results by Dohrmann and Widlund. The main result of the paper is a bound on the condition number of the algorithm which is cubic in the relative overlap and grows logarithmically with the number of elements across individual subdomains but is otherwise independent of the number of subdomains, their diameters and mesh sizes, and the incompressibility of the material and possible discontinuities of the material parameters across the subdomain interfaces. Numerical results in the plane confirm the theory and also indicate that an analogous result should hold for the saddle point formulation, as well as for spectral element discretizations.

Key words. almost incompressible linear elasticity, domain decomposition methods, two-level overlapping Schwarz preconditioners, saddle point problems, mixed finite and spectral elements

AMS subject classifications. 65F08, 65F10, 65N30, 65N55

1. Introduction. Finite element discretizations of linear elasticity problems, using only displacement variables, suffer increasingly from locking effects and ill-conditioning when materials approach the incompressible limit. A well-known remedy is to use mixed finite elements with both displacement and pressure variables, but this approach yields larger and indefinite discrete systems for which the design of scalable and efficient iterative solvers is quite challenging. In this paper, we construct and analyze overlapping Schwarz preconditioners for the almost incompressible elasticity system discretized by $Q_2^h - P_1^h$ mixed finite elements with discontinuous pressures on hexagonal elements both on the fine and the coarse level. The resulting discrete saddle point problem can be solved iteratively by GMRES with an overlapping Schwarz preconditioner based on solving local and coarse saddle point problems involving both displacements and pressures. Alternatively, since we use discontinuous pressure fields, we can eliminate the pressure variables on the element level and return to a positive definite, although extremely ill-conditioned, problem for which we can use PCG with a classical overlapping Schwarz preconditioner based on local and coarse positive def-

---

inite problems involving only the displacements.

We provide a full analysis for the positive definite approach, by exploring tools and results developed by Dohrmann and Widlund [9, 10] and Dryja, Sarkis and Widlund [13]. We believe that our theoretical result is the first for overlapping Schwarz methods of this kind which use conventional coarse problems rather than the more exotic spaces of Dohrmann and Widlund. Those spaces were borrowed from iterative substructuring methods; cf. [34, Chapter 5]. A key idea in the proof is to reduce the analysis to subspaces which satisfy a no-net flux condition across the interface between the subdomains. In fact, we will work with functions that satisfy this condition across each subdomain face which form the interface. Our main result is a bound on the condition number which is cubic in the relative overlap and grows logarithmically with the number of elements across individual subdomains but is otherwise independent of the number of subdomains, their diameters and mesh sizes, and the incompressibility of the material. Our result is also independent of possible discontinuities of the material parameters across the subdomain interfaces under an assumption of quasi-monotonicity, which was not required in the earlier work by Dohrmann and Widlund. Our analysis does not cover the approach based on a saddle point formulation but numerical results indicate that analogous results should hold even in that case.

The use of two-level overlapping Schwarz methods for saddle point problems, such as the mixed elasticity and Stokes systems, has previously been explored by Klawonn and Pavarino [21, 22]. These algorithms have been used, e.g., in computational fluid dynamics [18, 19], fluid-structure interaction [1], and isogeometric analysis [3]. In earlier work by Fischer [14], overlapping Schwarz methods have been studied for the pressure operator of the incompressible Navier-Stokes system discretized with spectral elements. Earlier studies on nonoverlapping domain decomposition algorithms for mixed elasticity and Stokes systems have focused on Wirebasket and Balancing Neumann-Neumann methods, see [29, 30, 17], [2], and on FETI-DP and BDDC methods for the incompressible limit, see [7], [24, 25], [23], [31], [20], [26, 35]. Some of these studies have already considered the positive definite reduction of the mixed almost incompressible elasticity system, namely [16], [2], [31], using Balancing Neumann-Neumann and BDDC methods, see also [9, 10] which use standard and hybrid overlapping Schwarz methods.

We note that while the positive definite reduction cannot be applied in the incompressible limit, we still could build a preconditioner for the Stokes system by using a preconditioner for a slightly compressible problem. We also note that in the more challenging case of continuous pressure approximations, some FETI-DP type algorithms have been developed and analyzed in pioneering work by Li and Tu [26, 35]. Dohrmann also has a version of the algorithm of [9] which performs virtually the same for discontinuous and continuous pressure approximations; so far a supporting theory is lacking.

Our algorithms apply equally well to hp and spectral element discretizations with discontinuous pressures. Indeed, we have also considered mixed spectral elements of the $Q_n - Q_{n-2}$ family, based on Gauss-Lobatto-Legendre quadrature and a nodal basis (see Bernardi and Maday [4]) and have found analogous numerical results; see Section 6. We remark that alternative preconditioners for almost incompressible materials might be developed directly for the pure displacement formulation when hp and spectral element methods are employed, since these higher order discretizations are known to eliminate locking without resorting to mixed formulations, see e.g. [32].

The rest of the paper is organized as follows. The almost incompressible elas-

ticity system and its mixed finite element discretization is introduced in Section 2. Overlapping Schwarz methods for the positive definite reformulation are introduced in Section 3, while analogous methods for the mixed formulation are given in Section 4. The theoretical analysis of our method for the positive definite formulation is provided in Section 5. Numerical results in the plane for both formulations are presented in Section 6.

2. Almost incompressible elasticity and mixed finite elements.

2.1. The continuous problem. We consider a domain $\Omega \subset R^d, d = 2, 3$, decomposed into N nonoverlapping subdomains Ω_i of diameter H_i, and forming a coarse finite element partition τ_H of Ω,

$$\overline{\Omega} = \bigcup_{i=1}^{N} \overline{\Omega}_i. \tag{2.1}$$

Let $H = \max_i H_i$ be the characteristic diameter of the subdomains and $\partial\Omega_D$ a nonempty subset of $\partial\Omega$. To simplify our discussion, we will only consider the case of $\partial\Omega_D = \partial\Omega$ and we will also assume that the solution vanishes on $\partial\Omega$. The interface of the domain decomposition (2.1) is given by

$$\Gamma = \left(\bigcup_{i=1}^{N} \partial\Omega_i \right) \setminus \partial\Omega.$$

In the next subsection, we will further partition each subdomain into many shape-regular finite elements. We will assume that the nodes match across the interface between the subdomains.

We consider a mixed formulation of linear elasticity for almost incompressible materials as, e.g., in [5]: find $(\boldsymbol{u}, p) \in \boldsymbol{V} \times U$ such that

$$\begin{cases} 2 \displaystyle\int_{\Omega} \mu \; \epsilon(\boldsymbol{u}) : \epsilon(\boldsymbol{v}) \; dx & - & \displaystyle\int_{\Omega} \operatorname{div} \boldsymbol{v} \; p \; dx & = & \langle \mathbf{F}, \boldsymbol{v} \rangle & \forall \boldsymbol{v} \in \boldsymbol{V}, \\[2mm] - \displaystyle\int_{\Omega} \operatorname{div} \boldsymbol{u} \; q \; dx & - & \displaystyle\int_{\Omega} \frac{1}{\lambda} \; pq \; dx & = & 0 & \forall q \in U. \end{cases} \tag{2.2}$$

The displacement and pressure spaces are given by

$$\boldsymbol{V} := \{ \boldsymbol{v} \in H^1(\Omega)^d : \boldsymbol{v}|_{\partial\Omega_D} = 0 \}, \quad U := L_0^2(\Omega) := \{ p \in L^2(\Omega), \int_{\Omega} p dx = 0. \}$$

$\mathbf{F}$ represents the applied forces and $\mu(x)$ and $\lambda(x)$ are the Lamé parameters of the material that, for simplicity, are assumed to be constant in each subdomain Ω_i, i.e. $\mu = \mu_i$ and $\lambda = \lambda_i$ in Ω_i. These parameters can be expressed in terms of the local Poisson ratio ν_i and Young's modulus E_i as

$$\mu_i := \frac{E_i}{2(1 + \nu_i)}, \qquad \lambda_i := \frac{E_i \nu_i}{(1 + \nu_i)(1 - 2\nu_i)}. \tag{2.3}$$

The material of a subdomain approaches the incompressible limit when $\nu_i \to 1/2$. Factoring out the constants μ_i and $\frac{1}{\lambda_i}$, we can define local bilinear forms in terms of

3

integrals over the subdomains Ω_i and obtain

$$a(\boldsymbol{u}, \boldsymbol{v}) = \sum_{i=1}^{N} \mu_i a_i(\boldsymbol{u}, \boldsymbol{v}) := 2 \sum_{i=1}^{N} \mu_i \int_{\Omega_i} \varepsilon(\boldsymbol{u}) : \varepsilon(\boldsymbol{v}) \ dx, \tag{2.4}$$

$$c(p, q) = \sum_{i=1}^{N} \frac{1}{\lambda_i} c_i(p, q) := \sum_{i=1}^{N} \frac{1}{\lambda_i} \int_{\Omega_i} p \ q \ dx, \tag{2.5}$$

$$b(\boldsymbol{v}, q) = \sum_{i=1}^{N} b_i(\boldsymbol{v}, q) := - \sum_{i=1}^{N} \int_{\Omega_i} \mathrm{div}\boldsymbol{v} \ q \ dx. \tag{2.6}$$

Thus, the global problem (2.2) can be obtained by assembling contributions to the bilinear forms from those of the subdomains.

2.2. $Q_2^h - P_1^h$ mixed finite elements with discontinuous pressures. We consider a fine triangulation τ_h of Ω obtained as a refinement of the coarse triangulation τ_H and discretize the continuous saddle point problem with $Q_2^h - P_1^h$ mixed finite elements. The displacement space consists of continuous, vector-valued, piecewise bi- or tri-quadratic functions:

$$\boldsymbol{V}^h := \{\boldsymbol{v} \in \boldsymbol{V} : \boldsymbol{v}|_T \in (Q_2^h(T))^d \ \ \forall T \in \tau_h\},$$

while the pressure space consists of discontinuous, scalar, piecewise linear functions with a zero average:

$$U^h := \{q \in U : q|_T \in P_1^h(T) \ \ \forall T \in \tau_h\}.$$

The two spaces are defined on the same quadrilateral or hexahedral mesh. This mixed finite element method satisfies a uniform inf-sup condition:

$$\sup_{\boldsymbol{v} \in \boldsymbol{V}^h} \frac{b_i(\boldsymbol{v}, q)}{a_i(\boldsymbol{v}, \boldsymbol{v})^{1/2}} \geq \beta c_i(q, q)^{1/2} \ \ \forall q \in U^h, \ \ \beta > 0. \tag{2.7}$$

For a proof of this result see Girault and Raviart [15, pp. 156–158].

We have also considered mixed spectral elements of the $Q_n - Q_{n-2}$ family, based on Gauss-Lobatto-Legendre quadrature and a nodal basis (see Bernardi and Maday [4]), and found analogous numerical results. In this paper, we will focus on the $Q_2^h - P_1^h$ finite element case.

2.3. The discrete system and its positive definite reformulation. The discrete system obtained from mixed finite elements is assembled from the saddle point matrices of the subdomains Ω_i :

$$\begin{bmatrix} \mu_i A_i & B_i^T \\ B_i & -\frac{1}{\lambda_i} C_i \end{bmatrix}, \tag{2.8}$$

where $\mu_i A_i, B_i$, and $1/\lambda_i \ C_i$ are the matrices associated with the local bilinear forms $\mu_i a_i(\cdot, \cdot), \ b_i(\cdot, \cdot)$, and $1/\lambda_i c_i(\cdot, \cdot)$ defined in (2.4), (2.5), and (2.6), respectively.

Since we are using discontinuous pressures, all pressure degrees of freedom can be eliminated, element by element, to obtain reduced positive definite stiffness matrices

$$\bar{A}_i := \mu_i A_i + \lambda_i B_i^T C_i^{-1} B_i, \tag{2.9}$$

that can be subassembled into a global, positive definite stiffness matrix $\bar{A}$. We denote the bilinear form associated to $\bar{A}$ by

$$\bar{a}(\boldsymbol{u}, \boldsymbol{v}) = \boldsymbol{u}^T \bar{A} \boldsymbol{v}.$$

The load vector of the full system can similarly be assembled from contributions from the subdomains. For further details see [9, Sections 2 and 3]. We note that we have to develop estimates using the bilinear forms $\bar{a}_i(\boldsymbol{u}_h, \boldsymbol{v}_h)$ in all our analysis and that they contain terms with the potentially huge factors λ_i. To control these terms, we will, when developing the theory, estimate $\bar{a}_i(\boldsymbol{u}_h - \boldsymbol{u}_0, \boldsymbol{u}_h - \boldsymbol{u}_0)$ instead of $\bar{a}_i(\boldsymbol{u}_0, \boldsymbol{u}_0)$ while making sure that the fluxes across the subdomain boundaries vanish:

$$\int_{\partial \Omega_i} \boldsymbol{w}_h \cdot \boldsymbol{n} \; ds = 0 \quad \text{where} \quad \boldsymbol{w}_h := \boldsymbol{u}_h - \boldsymbol{u}_0.$$

Here $\boldsymbol{u}_0 := I^H \boldsymbol{u}_h$, where I^H is an interpolant mapping onto a coarse space; see further Subsection 5.2. This no-net flux condition allows for a divergence free extension of the boundary data and we are then able to use [9, Lemma 3.3] to good effect obtaining the key estimate

$$\bar{a}_i(\boldsymbol{w}_h, \boldsymbol{w}_h) \le 4\mu_i(1 + \frac{d/2}{\mu_i/\lambda_i + \beta^2}) a_i(\boldsymbol{w}_h, \boldsymbol{w}_h). \tag{2.10}$$

Here β is the inf-sup parameter of the mixed finite element pair of spaces.

3. Overlapping Schwarz methods for the positive definite reformulation. We extend each subdomain Ω_i to a subdomain Ω_i', which will overlap other extended subdomains, by adding one or several layers of elements outside $\partial \Omega_i$. We will denote the minimal thickness of $\Omega_i' \setminus \Omega_i$ by δ_i. To each of the Ω_i', we then associate a local space

$$\boldsymbol{V}_i = \boldsymbol{V}^h(\Omega_i') \cap \boldsymbol{H}_0^1(\Omega_i')$$

and a bilinear form $\tilde{a}_i'(\boldsymbol{u}_i, \boldsymbol{v}_i)$. Since we will only consider algorithms for which the local problems are solved exactly, we find that $\tilde{a}_i'(\boldsymbol{u}_i, \boldsymbol{v}_i) := \bar{a}(R_i^T \boldsymbol{u}_i, R_i^T \boldsymbol{v}_i)$ where $R_i^T : \boldsymbol{V}_i \to \boldsymbol{V}^h$, simply extends any element of $\boldsymbol{V}_i$ by zero outside Ω_i'. We can also represent this bilinear form in terms of the principal minor $\bar{A}_i'$ of the matrix $\bar{A}$ associated with the degrees of freedom of the space $\boldsymbol{V}_i$.

We also define a coarse space $\boldsymbol{V}_0$ on the coarse subdomain mesh τ_H by

$$\boldsymbol{V}_0 = \boldsymbol{V}^H := \{\boldsymbol{v} \in \boldsymbol{V} : \boldsymbol{v}|_{\Omega_i} \in (Q_2^H(\Omega_i))^d \;\; \forall \Omega_i \in \tau_H\}.$$

We will also use a coarse embedding operator $R_0^T : \boldsymbol{V}_0 \to \boldsymbol{V}^h$; $R_0^T \boldsymbol{v}_0$ is simply the $\boldsymbol{V}^h$-interpolant of $\boldsymbol{v}_0 \in \boldsymbol{V}_0$.

The discrete space $\boldsymbol{V}^h$ can then be decomposed into a coarse and many local spaces as follows:

$$\boldsymbol{V}^h = R_0^T \boldsymbol{V}_0 + \sum_{i=1}^N R_i^T \boldsymbol{V}_i.$$

We next define local and coarse (for $i = 0$) operators $\widetilde{P}_i : \boldsymbol{V}^h \to \boldsymbol{V}_i$ by

$$\tilde{a}'(\widetilde{P}_i \boldsymbol{u}, \boldsymbol{v}_i) = \bar{a}(\boldsymbol{u}, R_i^T \boldsymbol{v}_i) \quad \forall \boldsymbol{v}_i \in \boldsymbol{V}_i.$$

5

Given that we are using exact solvers for all the subspaces, we find that $P_i := R_i^T \widetilde{P}_i :$ $\boldsymbol{V}^h \to \boldsymbol{V}^h$, are all projections; cf. [34, Section 2.2]. Our two-level Overlapping Additive Schwarz (OAS) operator is then given by

$$P_{OAS} := P_0 + \sum_{i=1}^{N} P_i. \tag{3.1}$$

The matrix form of this operator is $P_{OAS} = B_{OAS}\bar{A}$, where $\bar{A}$ is the stiffness matrix of the positive definite reformulation and B_{OAS} the Additive Schwarz preconditioner

$$B_{OAS} = R_0^T \bar{A}_0^{-1} R_0 + \sum_{i=1}^{N} R_i^T \bar{A}_i'^{-1} R_i. \tag{3.2}$$

Here, $\bar{A}_i' = R_i \bar{A} R_i^T$ are the local stiffness matrices associated with the subspace $\boldsymbol{V}_i$ and $\bar{A}_0 = R_0 \bar{A} R_0^T$ the coarse stiffness matrix. We can also define multiplicative and hybrid Schwarz preconditioners B_{OMS}, B_{OHS} as in [34, Section 2.2]. In some of our experiments, we will also consider one-level additive algorithms simply obtained by dropping in (3.1) the coarse term P_0, which originates from the coarse space $\boldsymbol{V}_0$.

4. Overlapping Schwarz methods for the mixed formulation. A related but different Overlapping Schwarz preconditioner can be constructed directly from the mixed formulation of the almost incompressible elasticity system. To this end, we define the local pressure spaces

$$U_i := \{q \in U^h : \int_{\Omega_i'} q = 0 \text{ and } q|_T = 0 \; \forall T \in \tau_h : \overline{T} \cap (\partial\Omega_i' \setminus \partial\Omega) \neq \emptyset\}.$$

We note that in order to satisfy the inf-sup condition of the local problems, the displacement space $\boldsymbol{V}_i$ should be sufficiently rich in relation to the pressure space U_i; given that we are working with overlapping subdomains, we have some flexibility when choosing the pressure spaces. Other variants of local pressure spaces could be considered as in [21, 28]; our choice in this paper corresponds to Version 2 in [21, 28]. This flexibility in choosing the local pressure spaces makes the saddle point preconditioner quite different from the positive definite preconditioner of the previous section.

A coarse pressure space is defined on the coarse subdomain mesh τ_H by

$$U_0 = U^H = \{q_0 \in U : q_0|_{\Omega_i} \in P_1^H(\Omega_i) \; \forall\Omega_i \in \tau_H\}.$$

Given local and coarse (for $i = 0$) embedding operators $R_i^{pT} : U_i \to U^h$, $i = 0, 1, .., N$, we can then decompose the discrete space $\boldsymbol{V}^h \times U^h$ into local and coarse spaces as

$$\boldsymbol{V}^h \times U^h = \sum_{i=0}^{N} (R_i^T \boldsymbol{V}_i \times R_i^{pT} U_i).$$

Define the local (for $i \geq 1$) operators $\widetilde{P}_i^m = \begin{bmatrix} \widetilde{P}_i^u \\ \widetilde{P}_i^p \end{bmatrix} : \boldsymbol{V}^h \times U^h \to \boldsymbol{V}_i \times U_i$ by

$$\begin{cases} a_i'(\widetilde{P}_i^u \boldsymbol{u}, \boldsymbol{v}) + b_i'(\boldsymbol{v}, \widetilde{P}_i^p p) = a(\boldsymbol{u}, R_i^T \boldsymbol{v}) + b(R_i^T \boldsymbol{v}, p) & \forall \boldsymbol{v} \in \boldsymbol{V}_i, \\ b_i'(\widetilde{P}_i^u \boldsymbol{u}, q) - c_i'(\widetilde{P}_i^p p, q) = b(\boldsymbol{u}, R_i^{pT} q) - c(p, R_i^{pT} q) & \forall q \in U_i, \end{cases} \tag{4.1}$$

6

where the bilinear forms on the left hand sides are defined by integrals over Ω_i'. The operators for the coarse space is defined similarly. Defining $P_i^m := \begin{bmatrix} P_i^u \\ P_i^p \end{bmatrix} = \begin{bmatrix} R_i^T \widetilde{P}_i^u \\ R_i^{pT} \widetilde{P}_i^p \end{bmatrix}$, $i = 0, 1, .., N$, our two-level Overlapping Additive Schwarz (OAS) operator formally has the same structure as before

$$P_{OAS}^m = P_0^m + \sum_{i=1}^{N} P_i^m. \tag{4.2}$$

Its matrix form is $P_{OAS}^m = B_{OAS}^m A^m$, with the mixed elasticity stiffness matrix A^m obtained by subassembling the local matrices (2.8) and with the mixed preconditioner

$$B_{OAS}^m = \begin{bmatrix} R_0^T R_0^{pT} \end{bmatrix} A_0^{m-1} \begin{bmatrix} R_0 \\ R_0^p \end{bmatrix} + \sum_{i=1}^{N} \begin{bmatrix} R_i^T R_i^{pT} \end{bmatrix} \begin{bmatrix} \mu_i A_i' & B_i'^T \\ B_i' & -\frac{1}{\lambda_i} C_i' \end{bmatrix}^{-1} \begin{bmatrix} R_i \\ R_i^p \end{bmatrix}, \tag{4.3}$$

where $A_0^m = \begin{bmatrix} R_0 \\ R_0^p \end{bmatrix} A^m \begin{bmatrix} R_0^T R_0^{pT} \end{bmatrix}$. We remark that this preconditioner leads to a system with complex eigenvalues in spite of the symmetry of both the original system and the preconditioner. The symmetry cannot be recovered as in the case of the previous section because now the preconditioner and the original system are indefinite. Therefore, in general, we no longer can employ the conjugate gradient method but must resort to a more general Krylov space method such as GMRES, see e.g. [34, Section C.6]. As before, we can also define multiplicative and hybrid Schwarz preconditioners B_{OMS}^m, B_{OHS}^m for the saddle point formulation.

5. Condition number bounds. We will now establish a scalable condition number bound for the overlapping Schwarz methods defined in Section 3 for the positive definite formulation. We recall that our coarse space is based on a coarse triangulation into cubic subdomains and that the coarse displacement space equals $(Q_2^H)^3$; we will only consider the three-dimensional case when developing the theory. Our results extend immediately to mixed finite element methods based on tetrahedra provided that the pressure space is based on discontinuous functions. We note that it is important for our arguments that there is at least one interior node for the displacement variable on each subdomain face.

We note that for scalar elliptic problems, technical tools were developed in [34, Subsection 3.5] for a case where the coarse space triangulation can cut through the mesh cells of the fine triangulation. In [34, Subsection 8.2], some of that work was extended to problems of compressible linear elasticity. All that work concerned constant coefficients only. In our current work, we will only assume that the Lamé parameters are constant in each subdomain Ω_i and that the set of Lamé parameters $\{\mu_i\}_1^N$ satisfies a *quasi-monotonicity* condition; see Assumptions 1 and 2 below. Just as in [9, 10], we will be able to hide, in a certain sense, the term of $\bar{a}_i(\boldsymbol{u}_h, \boldsymbol{v}_h)$ with the potentially very large factor λ_i.

5.1. The assumptions and the main result. The following assumption was introduced in [13, Section 5] in work on multi-level Schwarz algorithms for scalar elliptic problems; the role of the coefficient function for these elliptic problems will be played by the set of Lamé parameters $\{\mu_i\}$ for the case at hand.

ASSUMPTION 1. *For each subdomain vertex $\mathcal{V}$, let $\mathcal{N}_\mathcal{V}$ be the set of subdomains which have this vertex in common. Let $i_\mathcal{V}^{max}$ be the index of the subdomain in $\mathcal{N}_\mathcal{V}$*

with the largest μ_i. For any subdomain Ω_i in $\mathcal{N}_\mathcal{V}$, there should exist a path, passing exclusively through subdomain faces of this set of subdomains, from Ω_i to $\Omega_\mathcal{V}^{max}$ such that the values of the Lamé parameter μ_j are monotonely increasing along the path.

For any subdomain vertex $\mathcal{V}$ on $\partial\Omega$, the boundary of Ω, we assume, additionally, that the subdomain of $\mathcal{N}_\mathcal{V}$ with the largest Lamé parameter μ_i has a face which is a subset of $\partial\Omega$.

We note that we can relax these conditions, at the expense of an additional factor in the final result, by allowing a modest decrease when we pass from one subdomain to the next along the paths.

In turns out that we can also relax Assumption 1 in another way and we will adopt the following assumption:

ASSUMPTION 2. *Consider the same paths as in the previous assumption but relax the condition assuming only that for any subdomain Ω_j along the path from Ω_i to $\Omega_\mathcal{V}^{max}$, the Lamé parameter satisfies $\mu_j \geq \mu_i$.*

It will be important that the union $\widehat{\Omega}_i$ of the subdomains and subdomain faces for all such paths associated with all the subdomain vertices of a single subdomain form a domain for which Poincaré's and Korn's inequalities can be used; it is therefore important that the paths, introduced in the assumptions, always pass from one subdomain to another through a subdomain face.

Our main result concerns the case when the pressure variable has been eliminated as in Section 3.

THEOREM 5.1. *Let the set of Lamé parameters $\{\mu_i\}$ be quasimonotone in the sense of Assumption 2. Then the condition number of the additive Schwarz operator P_{ad} defined in (3.1) satisfies*

$$\kappa(P_{ad}) \leq C(H/\delta)^3(1 + \log(H/\delta))(1 + \log(H/h)),$$

where C is a constant independent of the number of subdomains, their diameters and mesh sizes, and which depends only on the number of colors required for the overlapping subdomains and the shape regularity of the elements and subdomains.

Here, as is customary, $H/\delta := \max_i H_i/\delta_i$ and $H/h := \max_i H_i/h_i$ where H_i, h_i denote the diameter and mesh size of Ω_i and δ_i measures the overlap of Ω_i' and its next neighbors.

Thus, our bound will essentially be proportional to $(H/\delta)^3$, just as in [9, 10]. Two of these factors originating from the inf-sup parameter and the inequality (2.10) and one from the bound in (5.13); for a further discussion of these matters, see [9].

Given that we are analyzing an overlapping Schwarz method, for which we can use exact solvers for the coarse and local subspaces, the only main challenge is to develop a bound on the parameter C_0^2 as in [34, Assumption 2.2]:

$$\bar{a}(R_0^T \boldsymbol{u}_0, R_0^T \boldsymbol{u}_0) + \sum_{i=1}^N \bar{a}_i'(R_i^T \boldsymbol{u}_i, R_i^T \boldsymbol{u}_i) \leq C_0^2 \bar{a}(\boldsymbol{u}, \boldsymbol{u}), \tag{5.1}$$

for some decomposition $\boldsymbol{u} = \sum_{i=0}^N R_i^T \boldsymbol{u}_i$. We recall that the local bilinear forms $\bar{a}_i'(\cdot, \cdot)$ have been defined in Section 3 by confining the integration to the set Ω_i'. We will bound separately the coarse and local components of (5.1).

5.2. A bound for the coarse component. An element of the Q_2^H finite element method in three dimensions has 27 nodes located at the subdomain vertices, at the midpoints of the subdomain edges, at the middle of the six faces of the cube, and at

the center of the element. Associated with each of these nodes are three displacement components. We will now construct the coarse space component $\boldsymbol{u}_0$ of the Schwarz subspace decomposition of (5.1) and estimate its norm indirectly by estimating the norm of $\boldsymbol{w}_h := \boldsymbol{u}_h - \boldsymbol{u}_0$ in terms of the norm of $\boldsymbol{u}_h$.

The element $\boldsymbol{u}_0$ is defined in two steps; the second will make the flux of $\boldsymbol{w}_h$ vanish across each subdomain boundary, which will allow for a divergence free extension into the interior of each subdomain. In this second step only the nodal values at the center of the subdomain faces are changed; using just one parameter for each subdomain face, we will make the flux of $\boldsymbol{w}_h$ across that face vanish. We will use the notation $I^H \boldsymbol{u}_h := \boldsymbol{u}_0$ with the operator I^H linear. We will develop such an interpolation operator which also works well for non-zero values on the boundary of Ω.

Given an arbitrary element $\boldsymbol{u}_h$, the value of $\boldsymbol{u}_0$ at a subdomain vertex $\mathcal{V}$ in the interior of Ω is given by the best $\boldsymbol{L}^2(\Omega_{\mathcal{V}}^{max})$-approximation of $\boldsymbol{u}_h$, by vector-valued functions with trilinear components; after having computed this function, we simply evaluate it at $\mathcal{V}$. For a subdomain vertex on $\partial\Omega$, we instead use the best approximation with respect to $\boldsymbol{L}^2(\mathcal{F})$, using the restriction of the same space of tri-linear functions to $\mathcal{F}$. Here, $\mathcal{F} := \partial\Omega_{\mathcal{V}}^{max} \cap \partial\Omega$.

The nodal values of the coarse components at the nodes that are not at vertices of the coarse elements are obtained by Q_1^H−interpolation, component by component, using the values at the subdomain vertices. We denote the resulting function by $\tilde{\boldsymbol{u}}_0$. This function, which belongs to $(Q_2^H)^3$, is finally corrected by changing the nodal values of the normal displacements at the center of all coarse element faces. The new values are chosen so that the integral of the normal component of $\boldsymbol{w}_h$ over any of these faces will vanish. Thus, we determine a correction term $\delta\boldsymbol{u}_0$ by the condition

$$\int_{\mathcal{F}} \boldsymbol{w}_h \cdot \boldsymbol{n}dA = \int_{\mathcal{F}} (\boldsymbol{u}_h - \tilde{\boldsymbol{u}}_0 - \delta\boldsymbol{u}_0) \cdot \boldsymbol{n}dA = 0. \tag{5.2}$$

Here $\mathcal{F}$ is any subdomain face of $\partial\Omega_i$ and $\boldsymbol{n}$ a vector normal to $\mathcal{F}$. The face correction term $(\delta\boldsymbol{u}_0)$ for this face equals $\alpha_{\mathcal{F}}\phi_c(x)\boldsymbol{n}$, where ϕ_c is the nodal basis function of Q_2^H associated with that node, which equals 1 at the center of the face, and which vanishes at all other nodes of the coarse triangulation. It is easy to see that $\int_{\mathcal{F}} \phi_c(x)dA$ is proportional to $|\mathcal{F}|$ and that $|\phi_c|^2_{\boldsymbol{H}^1(\Omega_i)} \leq C|\mathcal{F}|^{1/2} \leq CH_i$. To estimate α_F, we use equation (5.2), Cauchy-Schwarz's inequality, and an elementary trace theorem

$$\|\boldsymbol{f}\|^2_{\boldsymbol{L}^2(\mathcal{F})} \leq CH_i\|\boldsymbol{f}\|^2_{\boldsymbol{H}^1(\Omega_i)}, \; where \; \|\boldsymbol{f}\|^2_{\boldsymbol{H}^1(\Omega_i)} := |\boldsymbol{f}|^2_{\boldsymbol{H}^1(\Omega_i)} + H_i^{-2}\|\boldsymbol{f}\|^2_{\boldsymbol{L}^2(\Omega_i)}; \tag{5.3}$$

cf., e.g., [27]. We obtain the estimate $\|\delta\boldsymbol{u}_0\|^2_{\boldsymbol{H}^1(\Omega_i)} \leq C\|\boldsymbol{u}_h - \tilde{\boldsymbol{u}}_0\|^2_{\boldsymbol{H}^1(\Omega_i)}$ using that $\|\phi_c\|^2_{\boldsymbol{L}^2(\Omega_i)} \leq CH_i^3$. We will show below that $\|\boldsymbol{u}_h - \tilde{\boldsymbol{u}}_0\|_{\boldsymbol{H}^1(\Omega_i)} \leq C\|\boldsymbol{u}_h\|_{\boldsymbol{H}^1(\Omega_i)}$.

It is easy to see that $\tilde{\boldsymbol{u}}_0 = \boldsymbol{r}$ if $\boldsymbol{u}_h = \boldsymbol{r}$ for any element $\boldsymbol{r} \in \mathcal{RB}$, the space of rigid body modes. This follows from the fact that each component of a rigid body mode is a trilinear function. We also note that $\mathcal{RB}$ is the null space of the elasticity operator in the absence of boundary conditions. Thus, the *null space condition* is satisfied; cf. [33]. It is also true that $I^H\boldsymbol{r} = \boldsymbol{r}$ since $\boldsymbol{u}_h - \tilde{\boldsymbol{u}}_0$ will vanish already after the first step of our interpolation procedure if $\boldsymbol{u}_h \in \mathcal{RB}$. Therefore, the correction in the second step will also vanish.

We now turn to establishing the bound of $\boldsymbol{u}_h - \tilde{\boldsymbol{u}}_0$ in terms of $\boldsymbol{u}_h$. Using the definition of $\tilde{\boldsymbol{u}}_0$ and following [13], we find that for a subdomain vertex $\mathcal{V}$, in the interior of the domain Ω, we have

$$H_i^3|(\tilde{\boldsymbol{u}}_0 - \boldsymbol{r})(\mathcal{V})|^2 \leq C\|\boldsymbol{u}_h - \boldsymbol{r}\|^2_{\boldsymbol{L}^2(\Omega_{\mathcal{V}}^{max})}. \tag{5.4}$$

To see this, we recall that $\mathcal{V}$ is a node on the boundary of $\Omega_{\mathcal{V}}^{max}$. The trilinear, vector-valued function that approximates $\boldsymbol{u}_h - \boldsymbol{r}$ in this subdomain has a $\boldsymbol{L}^2(\Omega_{\mathcal{V}}^{max})$−norm that is bounded from above by that of $\boldsymbol{u}_h - \boldsymbol{r}$. In addition, the square of its nodal value at $\mathcal{V}$, times H_i^3, can be bounded by the square of the $\boldsymbol{L}^2$-norm of that linear function given that the mass matrix for the coarse, finite dimensional space is well-conditioned and its elements are on the order of H_i^3.

We then find that for a subdomain with all its vertices in the interior of Ω,

$$\mu_i|I^H(\boldsymbol{u}_h - \boldsymbol{r})|^2_{\boldsymbol{H}^1(\Omega_i)} \leq C\mu_i H_i^{-2} \sum_{\mathcal{V}\in\bar{\Omega}_i} \|\boldsymbol{u}_h - \boldsymbol{r}\|^2_{\boldsymbol{L}^2(\Omega_{\mathcal{V}}^{max})}. \tag{5.5}$$

This follows from (5.4) and a trivial estimate of the energy of the coarse basis functions. The right-hand side of this inequality can be estimated after adding non-negative terms, the squares of semi-norms, by

$$C\mu_i \sum_{\mathcal{V}\in\bar{\Omega}_i} \|\boldsymbol{u}_h - \boldsymbol{r}\|^2_{\boldsymbol{H}^1(\Omega_{\mathcal{V}}^{max})} \leq C\mu_i\|\boldsymbol{u}_h - \boldsymbol{r}\|^2_{\boldsymbol{H}^1(\widehat{\Omega}_i)}.$$

Here $\widehat{\Omega}_i$ is the union of all the subdomains of all the paths, of Assumptions 1 and 2, of the subdomain vertices of Ω_i.

For a subdomain vertex that lies on $\partial\Omega$, we will use the trace theorem (5.3) to estimate $H_i^{-1}\|\boldsymbol{u}_h - \boldsymbol{r}\|^2_{\boldsymbol{L}^2(\mathcal{F})}$ in terms of $\|\boldsymbol{u}_h - \boldsymbol{r}\|^2_{\boldsymbol{H}^1(\Omega_{\mathcal{V}}^{max})}$.

The contribution from such a subdomain vertex can indeed be estimated by $H_i^{-1}\|\boldsymbol{u}_h - \boldsymbol{r}\|^2_{\boldsymbol{L}^2(\mathcal{F})}$. Thus, the vector-valued function $\boldsymbol{v}(x)$, with bilinear components, which is the best approximation of $\boldsymbol{u}_h - \boldsymbol{r}$ in the $\boldsymbol{L}^2(\mathcal{F})$-sense, satisfies $\|\boldsymbol{v}\|_{\boldsymbol{L}^2(\mathcal{F})} \leq \|\boldsymbol{u}_h - \boldsymbol{r}\|_{\boldsymbol{L}^2(\mathcal{F})}$. By an argument about a mass matrix, now for functions of two independent variables, we find that $H_i^2|\boldsymbol{v}(\mathcal{V})|^2 \leq C\|\boldsymbol{u}_h - \boldsymbol{r}\|^2_{\boldsymbol{L}^2(\mathcal{F})}$. We next multiply this vertex value by the coarse nodal basis function of that vertex and compute the energy of the resulting function, which can be bounded by $CH_i^{-1}\|\boldsymbol{u}_h - \boldsymbol{r}\|^2_{\boldsymbol{L}^2(\mathcal{F})}$. The trace theorem (5.3) then gives us the bound $C\|\boldsymbol{u}_h - \boldsymbol{r}\|^2_{\boldsymbol{H}^1(\Omega_{\mathcal{V}}^{max})}$ of the same form as for the interior subdomain vertices.

We note that we have already shown how to estimate the correction term $\delta\boldsymbol{u}_0$ in terms of $\boldsymbol{u}_h - \tilde{\boldsymbol{u}}_0$. We can therefore conclude that $\mu_i\|\boldsymbol{w}_h\|^2_{\boldsymbol{H}^1(\Omega_i)} \leq C\mu_i\|\boldsymbol{u}_h - \boldsymbol{r}\|^2_{\boldsymbol{H}^1(\hat{\Omega}_i)}$.

In order to establish a bound for $\bar{a}_i(\boldsymbol{u}_h - \boldsymbol{u}_0, \boldsymbol{u}_h - \boldsymbol{u}_0)$, we will revisit and revise arguments in [9]. Since $I^H\boldsymbol{r} = \boldsymbol{r}$, $\forall\boldsymbol{r}\in\mathcal{RB}$, we find that $\boldsymbol{u}_0 - \boldsymbol{r} = I^H(\boldsymbol{u}_h - \boldsymbol{r})$ and that $\boldsymbol{w}_h = \boldsymbol{u}_h - \boldsymbol{r} - I^H(\boldsymbol{u}_h - \boldsymbol{r})$. We will use the shift with $\boldsymbol{r}$ when using a Korn's inequality

$$\inf_{\boldsymbol{r}\in\mathcal{RB}} \|\boldsymbol{u}_h - \boldsymbol{r}\|_{\boldsymbol{H}^1(\hat{\Omega}_i)} \leq C \sum_{\Omega_j\subset\hat{\Omega}_i} a_j(\boldsymbol{u}_h, \boldsymbol{u}_h); \tag{5.6}$$

cf. [9, Lemma 5.2]. We note that by Assumption 2, the Lamé parameters of all the subdomains which form $\widehat{\Omega}_i$ are at least equal to μ_i and that $\widehat{\Omega}_i$ allow us to use a Korn inequality; we note that we can find a path from any subdomain of $\widehat{\Omega}_i$ to any other such subdomain via Ω_i passing only through subdomain faces. Then [9, Lemma 5.2] provide a bound in terms of $a_j(\boldsymbol{u}_h, \boldsymbol{u}_h)$.

$$\inf_{\boldsymbol{r}\in\mathcal{RB}} \mu_i\|I^H(\boldsymbol{u}_h - \boldsymbol{r})\|^2_{\boldsymbol{H}^1(\Omega_i)} \leq C\mu_i \sum_{\Omega_j\subset\widehat{\Omega}_i} a_j(\boldsymbol{u}_h, \boldsymbol{u}_h) \leq C \sum_{\Omega_j\subset\widehat{\Omega}_i} \mu_j a_j(\boldsymbol{u}_h, \boldsymbol{u}_h). \tag{5.7}$$

Since $\boldsymbol{w}_h$ satisfies the no-net-flux condition, we can now use equation (2.10) to estimate $\bar{a}_i(\boldsymbol{w}_h, \boldsymbol{w}_h)$ by $\mu_i a_i(\boldsymbol{w}_h, \boldsymbol{w}_h)$, which in turn can be estimated by the left hand side of (5.7) and finally by the right hand side of (5.7). Thus,

$$\bar{a}_i(\boldsymbol{w}_h, \boldsymbol{w}_h) \leq C \sum_{\Omega_j \subset \widehat{\Omega}_i} \mu_j a_j(\boldsymbol{u}_h, \boldsymbol{u}_h). \tag{5.8}$$

Finally, we note that, trivially, $\mu_j a_j(\boldsymbol{u}_h, \boldsymbol{u}_h) \leq \bar{a}_j(\boldsymbol{u}_h, \boldsymbol{u}_h)$.

We also note that in contrast to the construction in [9], $\boldsymbol{w}_h$ will generally not vanish at the subdomain vertices. However, using [34, Formula (4.16)] and an elementary estimate of the energy of the nodal basis functions, we find that the energy of the component associated with a subdomain vertex can be bounded in a satisfactory way; see further the next subsection.

5.3. Local bounds. In the analysis of the local components $\boldsymbol{u}_i \in \boldsymbol{V}_i$, into which $\boldsymbol{w}_h$ will be decomposed, we can follow the analysis in [9, Section 5.3] quite closely. There will be very few complications and we will be able to follow the strategy of [9] of doing analysis on one subdomain at a time until the very end when we have to bring in our estimate of $\bar{a}_i(\boldsymbol{w}_h, \boldsymbol{w}_h)$, which is based on (5.8). In fact, we will find that some of our arguments are simpler than those in [9].

In the analysis, we will first localize $\boldsymbol{w}_h$ to the faces and edges of the subdomain Ω_i, find and estimate correction terms which will make each of these local terms have no net flux, and then use these local terms to construct contributions from Ω_i to $\boldsymbol{V}_i$ and the subspaces $\boldsymbol{V}_j$ associated with the subdomains which intersect Ω_i.

We note that in the beginning of [9, Section 5.3], we had to examine the construction of $\boldsymbol{u}_0$ quite closely in order to avoid introducing an additional, unnecessary factor $(1 + \log(H/h))$. Given that we have established a uniform bound for the norm of $\boldsymbol{w}_h$ in Subsection 5.2, this will not be necessary. Since $\boldsymbol{w}_h$ generally will not vanish at the subdomain vertices, we have to modify our argument slightly when we consider certain edge terms. This is accomplished by a simple modification of the cut-off functions associated with the subdomain edges.

Before we turn to the analysis of the local terms, we will recall a result on the effect of the aspect ratios of domains on the inf-sup parameter. We also will borrow a bound, from [9, Lemma 5.4], for certain face cutoff functions $\vartheta^\delta_{\mathcal{F}^{ij}}$ which are supported in the closure of the set

$$\Xi_{ij} := (\Omega_i \cup \mathcal{F}^{ij} \cup \Omega_j) \cap (\Omega'_i \cap \Omega'_j). \tag{5.9}$$

In addition, for each edge $\mathcal{E}^{j\ell} \subset \partial\Omega_i$, common to two faces $\mathcal{F}^{ij}$ and $\mathcal{F}^{i\ell}$ of Ω_i, we will consider a modified edge cutoff function, $\bar{\vartheta}^\delta_{\mathcal{E}^{j\ell}}$; it represents, in fact, a small modification of the function $\vartheta^\delta_{\mathcal{E}^{j\ell}}$ introduced in [9, Subsection 5.3]. This function is supported in the closure of the set

$$\Psi_{j\ell} := \bigcap_{m \in I_{j\ell}} \Omega'_m, \tag{5.10}$$

which is the intersection of the extensions Ω'_m of all subdomains Ω_m, which have the edge $\mathcal{E}^{j\ell}$ in common with Ω_i. Here the set of subdomain indices, denoted by $I_{j\ell}$, also includes i.

Bounds over these two sets of domains, which have aspect ratios of order H_i/δ_i, will affect the estimates of the $\boldsymbol{u}_i \in \boldsymbol{V}_i$, $i \geq 1$, in the decomposition which results

in our estimate of C_0^2. In contrast, these aspect ratios do not enter the bound of the coarse space component $\boldsymbol{u}_0$ since all estimates required in Section 5.2 are for entire subdomains which, by assumption, are shape regular.

The effect of the aspect ratio has been considered in the literature, in particular, by Dobrowolski [6]. These matters are discussed at some length in [9] where it is shown that the inf-sup constant of a domain such as Ξ_{ij} will decrease in proportion to δ_i/H_i. Using inequality (2.10) in an almost incompressible case will then contribute a factor $(H_i/\delta_i)^2$ to our bound of C_0^2.

A standard tool in the theory for iterative substructuring problems is provided by [34, Lemma 4.24]

$$|I^h(\vartheta_{\mathcal{F}^{ij}}\boldsymbol{u})|^2_{\boldsymbol{H}^1(\Omega_i)} \leq C(1 + \log(H_i/h_i))^2\|\boldsymbol{u}\|^2_{\boldsymbol{H}^1(\Omega_i)}. \tag{5.11}$$

Here $\vartheta_{\mathcal{F}^{ij}}$ is an explicitly constructed function, which equals 1 at all nodes interior to the face $\mathcal{F}^{ij}$. We also have the bound

$$|\vartheta_{\mathcal{F}^{ij}}|^2_{H^1(\Omega_i)} \leq C(1 + \log(H_i/h_i))H_i; \tag{5.12}$$

see [34, Lemma 4.25]. In our analysis of the local terms, we need similar bounds but for the intersection of Ω_i with Ω'_j, the extension of the other subdomain Ω_j, which has a face $\mathcal{F}^{ij}$ in common with Ω_i. Just as in [9], we will use a face cutoff function $\vartheta^\delta_{\mathcal{F}^{ij}}$ which is different from $\vartheta_{\mathcal{F}^{ij}}$ in two respects. Instead of having the value 1 at all nodes of $\mathcal{F}^{ij}$, it will equal $dist(x, \partial\mathcal{F}^{ij})/\delta_i$, at any node $x \in \mathcal{F}^{ij}$ within a distance δ_i of the boundary of the face; at all other nodes on $\mathcal{F}^{ij}$ the nodal values remain 1. We note that this function thus resembles a regular face cutoff function on a coarser mesh with elements of size δ_i. In addition, we will restrict the support of this cutoff function to the closure of Ξ_{ij}. The bound on the right-hand side of (5.11) must then be multiplied by a factor H_i/δ_i. On the other hand, one of the factors $(1+\log(H_i/h_i))$ in (5.11) can be replaced by $(1 + \log(H_i/\delta_i))$.

LEMMA 5.2. *There exists a face cutoff function $\vartheta^\delta_{\mathcal{F}^{ij}}$, with values at the nodes of $\mathcal{F}^{ij}$ as just specified, which vanishes at all the nodes on the rest of the boundary of $\Omega_i \cap \Omega'_j$, and which satisfies*

$$|I^h(\vartheta^\delta_{\mathcal{F}^{ij}}\boldsymbol{u})|^2_{\boldsymbol{H}^1(\Omega_i \cap \Omega'_j)} \leq C(H_i/\delta_i)(1 + \log(H_i/\delta_i))(1 + \log(H_i/h_i))\|\boldsymbol{u}\|^2_{\boldsymbol{H}^1(\Omega_i)}. \tag{5.13}$$

For a proof of this result see [9, Lemma 5.4].

The modified edge function $\bar{\vartheta}^\delta_{\mathcal{E}^{j\ell}}$ is supported in the closure of a δ_i-neighborhood of the subdomain edge $\mathcal{E}^{j\ell}$ and in the closure of $\Psi_{j\ell}$. The $\bar{\vartheta}^\delta_{\mathcal{E}^{j\ell}}$ of all the edges of Ω_i and the $\vartheta^\delta_{\mathcal{F}^{j\ell}}$ of all the faces of the subdomain should form a partition of unity when restricted to $\partial\Omega_i$. It is straightforward to construct such edge functions which satisfy $|\nabla\bar{\vartheta}^\delta_{\mathcal{E}^{j\ell}}| \leq C/\delta_i$. By introducing cylindrical coordinates, with the edge as the z-axis, and using [34, Corollary 4.20], we can prove the following; cf. [9, Lemma 5.5].

LEMMA 5.3. *There exist edge cutoff functions $\bar{\vartheta}^\delta_{\mathcal{E}^{j\ell}}$ supported in the closure of $\Psi_{j\ell}$, which, together with the face cutoff functions $\vartheta^\delta_{\mathcal{F}^{ik}}$ form a partition of unity on $\partial\Omega_i$ and which satisfies*

$$|I^h(\bar{\vartheta}^\delta_{\mathcal{E}^{j\ell}}\boldsymbol{u})|^2_{\boldsymbol{H}^1(\Psi_{j\ell})} \leq C(1 + \log(H_i/h_i))\|\boldsymbol{u}\|^2_{\boldsymbol{H}^1(\Omega_i)}. \tag{5.14}$$

We note that a proof, cited in the proof of this result, from [34, Lemma 4.16], is not satisfactory but that a good proof now is provided in [11, Lemma 3.1].

	saddle point GMRES-OAS(2)		saddle point GMRES-OHS(2)	
ν	it.	err.	it.	err.
0.4	16	5.8e-6	14	2.3e-6
0.49	18	3.8e-6	15	3.6e-6
0.499	18	6.5e-6	15	4.4e-6
0.4999	18	6.7e-6	15	4.5e-6
0.49999	18	6.8e-6	15	4.5e-6
0.499999	18	6.8e-6	15	4.5e-6

TABLE 6.1

Saddle point formulation. GMRES with two-level additive (OAS) and hybrid (OHS) precon-ditioners. Iteration counts and iteration errors for an increasing Poisson ratio $\nu \to \frac{1}{2}$. Fixed $N = 3 \times 3$, $H/h = 4$, overlap $\delta = h$.

Just as in [9, Subsection 5.3], these face and edge functions are used in order to partition $\boldsymbol{w}_h$ into functions that are supported in the closure of individual overlapping subdomains Ω'_j. However, while $\boldsymbol{w}_h$, by construction, has a zero net flux across all subdomain faces, this is no longer the case with the local functions just constructed. We therefore have to introduce correction terms and here we can follow [9] very closely. For each face $\mathcal{F}^{ij}$, we thus obtain a modified face function $\boldsymbol{w}_{\mathcal{F}^{ij}}$ and for each subdomain edge $\mathcal{E}^{i\ell}$ a modified edge function $\boldsymbol{w}_{\mathcal{E}^{i\ell}}$. All of these functions have zero net flux across the subdomain boundary $\partial\Omega_i$. In addition, these functions satisfy the same bounds as those of Lemmas 5.2 and 5.3. The sum of these face and edge functions also equals $\boldsymbol{w}_h$ on the interface.

What remains is to partition $\boldsymbol{w}_i$, the restriction of $\boldsymbol{w}_h$ to Ω_i, into contributions to the local subspace $\boldsymbol{V}_i$ and the subspaces associated with the subdomains which have a face or edge in common with Ω_i. Here we can exactly use the recipes of [9, Subsection 5.3]. Thus, we begin the construction of the restriction of $\boldsymbol{u}_i \in \boldsymbol{V}_i$ to Ω_i by subtracting $(1/2)\boldsymbol{w}_{\mathcal{F}^{ij}}$ from $\boldsymbol{w}_i$ and adding the same function to the restriction of $\boldsymbol{u}_j \in \boldsymbol{V}_j$ to the same subdomain Ω_i. By using the same recipe for the neighboring subdomain Ω_j we obtain an element in $\boldsymbol{V}_i$. A similar partitioning is also made of the edge functions $\boldsymbol{w}_{\mathcal{E}^{i\ell}}$; for details see [9, Subsection 5.3].

The conclusion of the proof of our main theorem can also very closely be modeled on that earlier work; see also the discussion at the end of Subsection 5.2.

6. Numerical results. In this section, we report on results of numerical tests in 2D with the Overlapping Additive Schwarz (OAS) preconditioners for the almost incompressible elasticity system as defined in Section 3 for the positive definite formulation and in Section 4 for the mixed formulation. Our problem is discretized with $Q_2^h - P_1^h$ mixed finite elements with the mesh size h. Analogous results have been obtained with $Q_n(h) - Q_{n-2}(h)$ spectral elements with polynomial degree n and with GLL numerical quadrature. At the end of this section, we report on only a few selected results for increasing polynomial degree n and Poisson ratio ν.

The domain is decomposed into N overlapping subdomains of characteristic size H and the overlap size δ is the minimal thickness of the extension $\Omega'_i \setminus \Omega_i$ of each subdomain Ω_i. The resulting linear system is solved by the GMRES method for the saddle point formulation and by the PCG method for the positive definite reformulation where the pressure has been eliminated. In all cases, we use one- or two-level overlapping Schwarz preconditioners as defined in Sections 3 and 4. The restart num-

	pos. definite formulation PCG-OAS(2)			pos. definite formulation PCG-OHS(2)		
ν	it.	err.	cond.=$\lambda_{max}/\lambda_{min}$	it.	err.	cond.=$\lambda_{max}/\lambda_{min}$
0.4	17	6.2e-7	5.61=4.788/0.854	14	4.1e-7	4.69=3.996/0.853
0.49	22	5.9e-7	10.88=4.822/0.443	17	3.2e-7	6.22=3.999/0.643
0.499	28	2.0e-7	23.31=4.842/0.208	25	1.2e-7	15.79=4.000/0.253
0.4999	36	5.8e-8	42.89=4.856/0.113	31	6.1e-8	29.88=4.000/0.134
0.49999	37	2.8e-8	47.68=4.859/0.102	32	5.2e-8	38.44=4.000/0.104
0.499999	38	1.1e-8	48.22=4.860/0.101	33	1.7e-8	39.61=4.000/0.101

TABLE 6.2

Positive definite formulation. PCG with two-level preconditioners: additive (OAS(2)) and hybrid (OHS(2)). Iteration counts, iteration errors, condition numbers and extreme eigenvalues for an increasing Poisson ratio $\nu \to \frac{1}{2}$. Fixed $N = 3 \times 3$, $H/h = 4$, overlap $\delta = h$.

ber of the GMRES method is set to be 200. We have run our Matlab program on a Linux PC, using a zero initial guess and a stopping criterion of a 10^{-6} reduction of the residual norm. In each test, we report the iteration counts (it.), the iteration errors (err.), i.e., the difference between the iterative solution and the solution obtained by using Matlab default direct solver and for PCG we also report the condition number (cond.) of the preconditioned operator defined as the ratio of its extreme eigenvalues $\lambda_{max}/\lambda_{min}$.

Robustness of OAS(2) and OHS(2) for almost incompressible materials. We first consider the saddle point formulation solved by GMRES with two-level additive (OAS) and hybrid (OHS) preconditioners. The system is discretized with a fixed number $N = 3 \times 3$ of subdomains, the ratio $H/h = 4$, and and an overlap $\delta = h$. Table 6.1 reports the iteration counts and errors of this saddle point system. The results clearly show the robustness of both OAS(2) and OHS(2) preconditioners when the Poisson ratio ν approaches the incompressible limit $\nu = \frac{1}{2}$, with a slightly better performance of the hybrid OHS(2) preconditioner.

Analogous results are shown in Table 6.2 for the positive definite formulation solved by PCG with two-level additive (OAS) and hybrid (OHS) preconditioners. Now we also report the condition numbers and extreme eigenvalues of the preconditioned operator. Again, the OHS(2) preconditioner has a slightly better performance due mostly to an smaller, largest eigenvalue.

Scalability of OAS(2). We then investigate the scalability of our overlapping Schwarz preconditioners. In Table 6.3, we consider both the two-level GMRES-OAS(2) and one-level GMRES-OAS(1) algorithms, applied to both the saddle point (top) and positive definite (bottom) formulations, for increasing number of subdomains N and a fixed $H/h = 5, \nu = 0.4999$. In each case, we consider both a minimal overlap of $\delta = h$ and a larger overlap of $\delta = 2h$. The results show that the GMRES-OAS(2) iteration count is bounded from above by a constant independent of N, clearly showing the scalability of the proposed preconditioners, while the one-level algorithm GMRES-OAS(1) is not scalable since its iteration count grows with N. Increasing the overlap size yields a considerable improvement for the positive definite formulation, but only a marginal improvement for the saddle point formulation. An analogous scalability test is reported in Table 6.4 for PCG-OAS(2) applied to the positive definite formulation with fixed $H/h = 5, \nu = 0.4999$, overlap $\delta = h$ (left) and $\delta = 2h$ (right), for N increasing up to 10×10 subdomains. We also report the condition numbers and extreme eigenvalues of the preconditioned operator.

| | saddle point, GMRES-OAS(2) | | | | saddle point, GMRES-OAS(1) | | | |
| | $\delta = h$ | | $\delta = 2h$ | | $\delta = h$ | | $\delta = 2h$ | |
N	it.	err.	it.	err.	it.	err.	it.	err.
2×2	16	4.8e-6	16	3.9e-6	19	6.6e-6	17	3.0e-6
3×3	19	5.5e-6	18	7.1e-6	29	1.4e-5	23	1.3e-5
4×4	20	7.7e-6	19	1.0e-5	39	1.9e-5	30	1.7e-5
5×5	20	1.1e-5	20	1.2e-5	50	3.2e-5	37	1.5e-5
6×6	21	7.4e-6	20	1.8e-5	63	3.7e-5	45	2.8e-5
	pos. definite, GMRES-OAS(2)				pos. definite, GMRES-OAS(1)			
2×2	24	1.4e-6	16	9.3e-7	21	8.8e-7	14	9.5e-7
3×3	39	2.5e-6	22	1.1e-6	35	1.9e-6	21	4.2e-7
4×4	44	7.5e-6	25	3.8e-6	61	1.6e-5	29	4.1e-6
5×5	43	3.1e-5	24	4.3e-6	84	3.4e-5	41	4.0e-6
6×6	43	1.7e-5	24	4.5e-6	115	2.0e-5	53	6.6e-6

TABLE 6.3

Scalability of GMRES-OAS(2), saddle point and positive definite formulations. Iteration counts and iteration errors for an increasing number of subdomains N. Fixed $H/h = 5$, $\nu = 0.4999$.

| positive definite formulation, PCG-OAS(2) | | | | | | |
| | $\delta = h$ | | | $\delta = 2h$ | | |
N	it.	err.	cond.=$\lambda_{max}/\lambda_{min}$	it.	err.	cond.=$\lambda_{max}/\lambda_{min}$
2×2	28	1.6e-8	63.99=4.655/0.073	19	9.1e-8	13.77=4.914/0.357
3×3	43	1.1e-7	68.82=4.767/0.069	26	3.0e-7	15.74=4.970/0.316
4×4	55	2.8e-7	63.91=4.794/0.075	30	1.4e-7	16.62=4.984/0.300
5×5	56	2.8e-7	62.31=4.804/0.077	30	1.7e-7	15.87=4.987/0.314
6×6	57	2.3e-7	61.40=4.809/0.078	30	2.0e-7	15.06=4.987/0.331
7×7	57	3.5e-7	60.17=4.810/0.080	30	2.8e-7	15.43=4.989/0.323
8×8	57	3.3e-7	57.95=4.811/0.083	30	2.2e-7	15.44=4.990/0.323
9×9	58	3.2e-7	56.75=4.813/0.085	30	2.9e-7	15.11=4.991/0.330
10×10	57	4.5e-7	58.79=4.814/0.082	30	4.1e-7	15.16=4.992/0.329

TABLE 6.4

Scalability of PCG-OAS(2), positive definite formulation. Iteration counts, iteration errors, condition numbers and extreme eigenvalues for increasing number of subdomains N. Fixed $H/h = 5$, $\nu = 0.4999$.

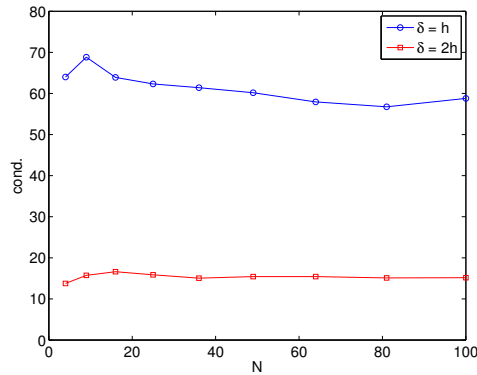FIG. 6.1. *Plot of cond. from Table 6.4.*

			positive definite formulation, PCG-OAS(2)			
		$\delta = h$			$\delta = 2h$	
H/h	it.	err.	cond.$=\lambda_{max}/\lambda_{min}$	it.	err.	cond.$=\lambda_{max}/\lambda_{min}$
4	16	1.3e-6	5.36=4.781/0.892	16	7.7e-7	4.95=4.976/1.005
5	17	1.1e-6	5.83=4.671/0.801	16	7.6e-7	4.94=4.942/0.999
6	17	1.3e-6	6.32=4.573/0.724	16	1.5e-6	4.97=4.894/0.984
7	18	1.9e-6	6.93=4.491/0.648	16	2.0e-6	5.16=4.839/0.939
8	18	3.2e-6	7.48=4.423/0.591	16	3.2e-6	5.37=4.782/0.891
16	23	8.9e-6	12.82=4.159/0.324	18	7.8e-6	7.51=4.425/0.589
24	27	1.2e-5	17.85=4.080/0.229	21	1.1e-5	9.82=4.250/0.433
32	30	2.5e-5	22.47=4.047/0.180	23	2.6e-5	12.36=4.160/0.337

TABLE 6.5

H/h-dependence of PCG-OAS(2), positive definite formulation. Iteration counts, iteration errors, condition numbers and extreme eigenvalues for increasing H/h. Fixed $N = 3 \times 3$, $\nu = 0.3$.

			positive definite formulation, PCG-OAS(2)			
		$\delta = h$			$\delta = 2h$	
H/h	it.	err.	cond.$=\lambda_{max}/\lambda_{min}$	it.	err.	cond.$=\lambda_{max}/\lambda_{min}$
4	36	5.8e-8	42.89=4.856/1.1e-1	22	1.3e-7	9.87=4.985/5.1e-1
5	43	1.1e-7	68.82=4.767/6.9e-2	26	3.0e-8	15.74=4.970/3.2e-1
6	50	1.6e-7	99.11=4.684/4.7e-2	28	1.3e-7	23.12=4.936/2.1e-1
7	57	2.8e-7	131.34=4.608/3.5e-2	33	1.3e-7	32.20=4.897/1.5e.1
8	64	2.7e-7	163.19=4.542/2.8e-2	37	1.6e-7	42.95=4.854/1.1e-1
16	117	1.4e-6	509.50=4.240/8.3e-3	64	8.8e-7	163.28=4.542/2.8e-2
24	144	3.5e-6	751.03=4.130/5.5e-3	87	4.1e-6	321.18=4.350/1.4e-2
32	163	8.3e-6	850.42=4.080/4.8e-3	109	4.5e-6	509.62=4.240/8.3e-3

TABLE 6.6

H/h-dependence of PCG-OAS(2), positive definite formulation. Iteration counts, iteration errors, condition numbers and extreme eigenvalues for increasing H/h. Fixed $N = 3 \times 3$, $\nu = 0.4999$.
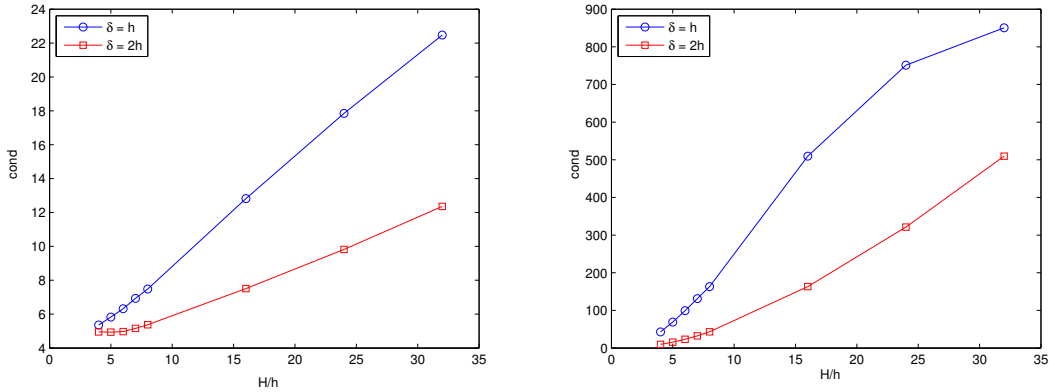

FIG. 6.2. *Plot of PCG-OAS(2) condition numbers from Table 6.5 with $\nu = 0.3$ (left) and from Table 6.6 with $\nu = 0.4999$ (right).*

	positive definite formulation, PCG-OAS(2)			
	$\nu = 0.3$		$\nu = 0.4999$	
H/δ	it.	cond.$=\lambda_{max}/\lambda_{min}$	it.	cond.$=\lambda_{max}/\lambda_{min}$
5.33	16	5.57=4.530/0.814	27	74.3=4.624/6.23e-2
6.40	17	5.92=4.437/0.750	31	112.1=4.535/4.05e-2
8.00	18	7.11=4.333/0.610	34	180.5=4.429/2.45e-2
10.67	20	8.97=4.222/0.470	45	305.0=4.305/1.41e-2
16.00	22	12.34=4.116/0.334	64	496.1=4.172/8.43e-3
21.33	25	15.74=4.070/0.259	80	590.7=4.108/7.00e-3
32.00	28	22.47=4.033/0.180	108	839.9=4.053/4.80e-3
42.67	31	29.22=4.019/0.138	158	1831.1=4.031/2.20e-3
64.00	36	42.75=4.009/0.094	229	4985.1=4.014/8.05e-4
128.00	47	83.37=4.002/0.048	475	22907.0=4.004/1.75e-4

TABLE 6.7

H/δ-dependence of PCG-OAS(2), positive definite formulation. Iteration counts, condition numbers and extreme eigenvalues for increasing H/δ. Fixed $N = 2 \times 2$, $H/h = 128$, $\nu = 0.3$ (left), $\nu = 0.4999$ (right).
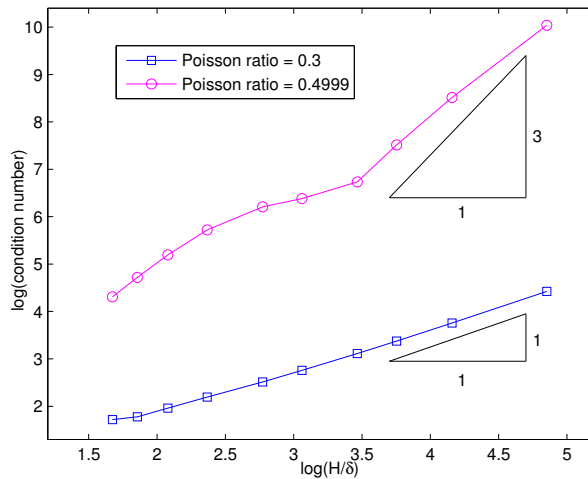

FIG. 6.3. *Plot of PCG-OAS(2) condition numbers from Table 6.7.*

All the results clearly show the scalability of PCG-OAS(2), in agreement with our main bound of Theorem 5.1. The condition numbers from this table are also plotted in Fig. 6.1 as a function of N.

OAS(2) dependence on H/h. We now investigate the OAS(2) dependence on the ratio H/h for the positive definite formulation, considering both a compressible material with $\nu = 0.3$ in Table 6.5 and an almost incompressible material with $\nu = 0.4999$ in Table 6.6. The number of subdomains is fixed to $N = 3 \times 3$, the overlap size is either $\delta = h$ (left) or $\delta = 2h$ (right), while the ratio H/h increases from 4 to 32. The PCG-OAS(2) condition numbers from both tables are also plotted in Fig. 6.2. The results indicate a growth of the condition number that in the compressible case seems to be linear in H/h. In the almost incompressible case, the condition numbers are much larger and their growth seems to be more than linear in H/h, even if for small

	GMRES-unpr.		GMRES-OAS(2)				PCG-OAS(2)		
	saddle pt.		saddle pt.		pos. def.		pos. def.			
ν	it.	err.	it.	err.	it.	err.	it.	err.	cond.=$\lambda_{max}/\lambda_{min}$	
	central jump test									
0.3	3+92	6e-2	15	5e-6	13	7e-9	17	9e-11	5.43=4.83/0.89	
0.4	3+99	0.34	16	4e-6	13	6e-9	17	9e-11	5.44=4.83/0.89	
0.49	4+108	1.8	17	1e-5	15	9e-9	20	2e-10	8.37=4.88/0.58	
0.499	4+110	2.1	17	1e-5	17	8e-9	24	3e-11	11.02=4.90/0.45	
0.4999	4+110	2.1	17	2e-5	17	2e-8	25	3e-11	11.58=4.91/0.42	
0.49999	4+110	2.1	17	2e-5	17	1e-8	25	3e-11	11.65=4.91/0.42	
	checkerboard test									
	8+116	2.5	17	1e-5	21	5e-9	31	1e-11	11.63=4.89/0.42	

TABLE 6.8

$Q_2^h - P_1^h$ *elements: discontinuous material parameters. OAS(2) iteration counts (number of restarts + number of iterations), iteration errors, (and also cond. and extreme eigenvalues for PCG-OAS(2)) for central jump and random jump tests. Fixed $N = 4 \times 4, H/h = 4$, overlap $\delta = h$.*

overlap $\delta = h$ the growth slows down for the larger values of $H/h = 24$ and 32. In all cases, this growth is due to the minimum eigenvalues decreasing toward zero when H/h increases. Also in all cases, a larger overlap improves the results considerably.

OAS(2) dependence on H/δ. In order to check our main bound in Theorem 5.1 predicting a $(H/\delta)^3$ growth of the condition number, we have investigated the effect of increasing the ratio H/δ while fixing $N = 4$ and $H/h = 128$. The results are reported in Table 6.7 and also plotted in Fig. 6.3 and appear to confirm the theoretical $(H/\delta)^3$ bound in the almost incompressible case, while the bound appear to be only linear in H/δ in the compressible case.

OAS(2) robustness with respect to discontinuous material parameters. In Table 6.8, we consider two tests with discontinuous material parameters. The first, called "central jump" (top part of the table), consists of a square domain with 4×4 subdomains, where the Poisson ratio ν equals the value given in the left column of the table in the 2×2 central subdomains, while $\nu = 0.3$ in the remaining subdomains. In the second test, called "checkerboard", the Poisson ratio is a piecewise constant function on each subdomain, with values varying randomly between 0.3 and 0.49999. From left to right, the table reports the iteration counts (number of restarts + number of iterations, so that e.g. $3 + 29$ means $3 \cdot 200 + 29$ iterations) and iteration errors of the unpreconditioned GMRES, GMRES-OAS(2) for the saddle point formulation, GMRES-OAS(2) for the positive definite formulation and PCG-OAS(2) for the positive definite formulation, where we report also the condition number and extreme eigenvalues. The results clearly show the OAS(2) robustness with respect to the jumps in the Poisson ratio in both the central jump and checkerboard tests, while the unpreconditioned GMRES does not converge in spite of large iteration counts with several restarts.

$Q_n - Q_{n-2}$ spectral elements: PCG-OAS(2) dependence on n and discontinuous material parameters. Finally, we remark that analogous results have been obtained with $Q_n - Q_{n-2}$ spectral element discretizations. Here, we only briefly report in Table 6.9 on the independence of the iteration count for PCG-OAS(2) of the polynomial degree n when the overlap size is at least one element. This is as expected from our previous studies on Schwarz preconditioners for spectral elements. Table

		positive definite formulation, PCG-OAS(2)				
		$\delta = h$			$\delta = 2h$	
n	it.	err.	cond.$=\lambda_{max}/\lambda_{min}$	it.	err.	cond.$=\lambda_{max}/\lambda_{min}$
3	37	6e-8	42.83=4.85/0.113	22	2e-7	9.87=4.99/0.506
4	37	1e-7	42.97=4.85/0.113	22	2e-7	9.88=4.99/0.505
5	36	2e-7	42.96=4.85/0.113	22	2e-7	9.86=4.98/0.505
6	36	5e-7	42.96=4.85/0.113	22	3e-7	9.88=4.99/0.505

TABLE 6.9

$Q_n - Q_{n-2}$ *spectral elements: n-dependence of PCG-OAS(2), positive definite formulation. Iteration counts, iteration errors, condition numbers and extreme eigenvalues for increasing polynomial degree n. Fixed $N = 3 \times 3, H/h = 4, \nu = 0.4999$.*

	GMRES-unpr.		GMRES-OAS(2)				PCG-OAS(2)		
	saddle pt.		saddle pt.		pos. def.		pos. def.		
ν	it.	err.	it.	err.	it.	err.	it.	err.	cond.$=\lambda_{max}/\lambda_{min}$
	central jump test								
0.3	1+132	3e-3	14	3e-7	13	5e-10	16	1e-10	5.41=4.81/0.89
0.4	2+87	4e-3	15	6e-7	13	2e-10	16	1e-10	5.48=4.82/0.74
0.49	4+81	1e-2	18	6e-6	14	4e-10	18	2e-10	6.50=4.84/0.74
0.499	4+94	2e-2	18	1e-6	17	2e-10	20	1e-10	8.17=4.91/0.60
0.4999	4+97	2e-2	18	2e-6	17	5e-10	22	7e-11	9.27=7.56/0.53
0.49999	4+98	1e-2	18	2e-6	17	6e-10	25	1e-11	9.98=4.93/0.49
	checkerboard test								
	10+0	1e-1	18	2e-6	19	3e-10	26	3e-11	11.52=4.90/0.42

TABLE 6.10

$Q_n - Q_{n-2}$ *spectral elements: discontinuous material parameters. OAS(2) iteration counts (number of restarts + number of iterations), iteration errors, (and also cond. and extreme eigenvalues for PCG-OAS(2)) for central jump and random jump tests. Fixed $n = 2, N = 4 \times 4, H/h = 4$, overlap $\delta = h$.*

6.10 shows the robustness of the OAS(2) algorithm in central jump and checkerboard tests, with results remarkably similar to the results of Table 6.8 for $Q_2^h - P_1^h$ elements.

REFERENCES

[1] A. T. BARKER AND X.-C. CAI, *Two-level Newton and hybrid Schwarz preconditioners for fluid-structure interaction*, SIAM J. Sci. Comp., 32 (2010), pp. 2395–2417.

[2] L. BEIRÃO DA VEIGA, C. LOVADINA AND L. F. PAVARINO, *Positive definite balancing Neumann-Neumann preconditioners for nearly incompressible elasticity*, Numer. Math., 104 (2006), pp. 271–296.

[3] L. BEIRÃO DA VEIGA, D. CHO, L. F. PAVARINO, S. SCACCHI, *Isogeometric Schwarz preconditioners for linear elasticity systems*, Comp. Meth. Appl. Mech. Engrg., 253 (2013), pp. 439–454.

[4] C. BERNARDI AND Y. MADAY, *Spectral Methods*, in *Handbook of Numerical Analysis, Volume V: Techniques of Scientific Computing (Part 2)*, P. G. Ciarlet and J.-L. Lions, editors, North-Holland, 1997, pp. 209–485.

[5] F. BREZZI AND M. FORTIN, *Mixed and hybrid finite element methods*. vol. 15 of Springer Series in Computational Mathematics, Springer-Verlag, Berlin Heidelberg New York, 1991.

[6] M. DOBROWOLSKI, *On the LBB constant on stretched domains*, Math. Nachr., 254–255:64–67, 2003.

[7] C. R. DOHRMANN, *A Substructuring Preconditioner for Nearly Incompressible Elasticity Problems*, Tech. Rep. SAND2004-5393, Sandia National Laboratories, (2004).

[8] C. R. Dohrmann, A. Klawonn, and O. B. Widlund, *A family of energy minimizing coarse spaces for overlapping Schwarz preconditioners*, in Proceedings of the 17th International Conference on Domain Decomposition Methods in Science and Engineering, held in Strobl, Austria, July 3-7, 2006, U. Langer, M. Discacciati, D. Keyes, O. Widlund, and W. Zulehner, eds., no. 60 in Springer-Verlag, Lecture Notes in Computational Science and Engineering, 2007, pp. 247–254.

[9] C. R. Dohrmann and O. B. Widlund, *An overlapping Schwarz algorithm for almost incompressible elasticity*, SIAM J. Numer. Anal., 47 (2009), pp. 2897–2923.

[10] C. R. Dohrmann and O. B. Widlund, *A hybrid domain decomposition method for compressible and almost incompressible elasticity*, Inter. J. Numer. Methods Engrg., 82 (2010), pp. 157–183.

[11] C. R. Dohrmann and O. B. Widlund, *A BDDC algorithm with deluxe scaling for three-dimensional H(curl) problems*, Tech. Report TR2014-964, Courant Institute, New York University, March 2014.

[12] M. Dryja, B. F. Smith, and O. B. Widlund, *Schwarz analysis of iterative substructuring algorithms for elliptic problems in three dimensions.* SIAM J. Numer. Anal., 31(6):1662–1694, 1994.

[13] M. Dryja, M. V. Sarkis, and O. B. Widlund, *Multilevel Schwarz methods for elliptic problems with discontinuous coefficients in three dimensions*, Numer. Math., 72 (1996), pp. 313–348.

[14] P. F. Fischer, *An overlapping Schwarz method for spectral element solution of the incompressible Navier–Stokes equations*, J. Comput. Phys., 133 (1997), pp. 84–101.

[15] V. Girault, P.-A. Raviart, *Finite element methods for Navier-Stokes equations. Theory and algorithms.* vol. 5 of Springer Series in Computational Mathematics, Springer-Verlag, Berlin Heidelberg New York, 1986.

[16] P. Goldfeld. *Balancing Neumann-Neumann preconditioners for the mixed formulation of almost-incompressible linear elasticity.* Technical Report TR2003-847, Courant Institute of Mathematical Sciences, NYU, 2003.

[17] P. Goldfeld, L. F. Pavarino, and O. B. Widlund, *Balancing Neumann-Neumann preconditioners for mixed approximations of heterogeneous problems in linear elasticity*, Numer. Math., 95 (2003), pp. 283–324.

[18] F. N. Hwang and X.-C. Cai, *A parallel nonlinear additive Schwarz preconditioned inexact Newton algorithm for incompressible Navier-Stokes equations*, J. Comp. Phys., 204 (2005), pp. 666–691.

[19] F. N. Hwang and X.-C. Cai, *A class of parallel two-level nonlinear Schwarz preconditioned inexact Newton algorithms*, Comput. Methods Appl. Mech. Engrg., 196 (2007), pp. 1603–1611.

[20] H. H. Kim and C.-O. Lee, *A two-level nonoverlapping Schwarz algorithm for the Stokes problem without primal pressure unknowns*, Internat. J. Numer. Methods Engrg., 88 (2011), pp. 1390–1410.

[21] A. Klawonn and L. F. Pavarino, *Overlapping Schwarz methods for mixed linear elasticity and Stokes problems*, Comput. Methods Appl. Mech. Engrg., 165 (1998), pp. 233–245.

[22] ———, *A comparison of overlapping Schwarz methods and block preconditioners for saddle point problems*, Numer. Lin. Alg. Appl., 7 (2000), pp. 1–25.

[23] A. Klawonn, O. Rheinbach, and B. Wohlmuth, *Dual-primal iterative substructuring for almost incompressible elasticity*, in Domain decomposition methods in science and engineering XVI, vol. 55 of Lect. Notes Comput. Sci. Eng., Springer, Berlin, 2007, pp. 397–404.

[24] J. Li, *A dual-primal FETI method for incompressible Stokes equations*, Numer. Math., 102 (2005), pp. 257–275.

[25] J. Li and O. B. Widlund, *BDDC algorithms for incompressible Stokes equations*, SIAM J. Numer. Anal., 44 (2006), pp. 2432–2455.

[26] J. Li and X. Tu, *A nonoverlapping domain decomposition method for incompressible Stokes equations with continuous pressures*, SIAM J. Numer. Anal., 51 (2013), pp. 1235–1253.

[27] J. Nečas, *Les méthodes directes en théorie des équations elliptiques*, Academia, 1967.

[28] L. F. Pavarino, *Indefinite overlapping Schwarz methods for time-dependent Stokes problems*, Comput. Methods Appl. Mech. Engrg., 187 (2000), pp. 35–51.

[29] L. F. Pavarino and O. B. Widlund, *Iterative substructuring methods for spectral element discretizations of elliptic systems. II. Mixed methods for linear elasticity and Stokes flow*, SIAM J. Numer. Anal., 37 (2000), pp. 375–402.

[30] L. F. Pavarino and O. B. Widlund, *Balancing Neumann-Neumann methods for incompressible Stokes equations*, Comm. Pure Appl. Math., 55 (2002), pp. 302–335.

[31] L. F. Pavarino, O. B. Widlund, S. Zampini, *BDDC preconditioners for spectral element dis-*

cretizations of almost incompressible elasticity in three dimensions, SIAM J. Sci. Comput., 32 (2010), pp. 3604–3626.

[32] Y. T. Peet and P. F. Fischer, *Legendre spectral element method with nearly incompressible materials*, Europ. J. Mech. Solid. 44 (2014), pp. 91–103.

[33] B. F. Smith, P. Bjørstad, and W. Gropp, *Domain Decomposition: Parallel Multilevel Methods for Elliptic Partial Differential Equations*, Cambridge University Press, New York, 1996.

[34] A. Toselli and O. B. Widlund, *Domain Decomposition Methods - Algorithms and Theory*, vol. 34 of Springer Series in Computational Mathematics, Springer-Verlag, Berlin Heidelberg New York, 2005.

[35] X. Tu and J. Li, *A unified dual-primal finite element tearing and interconnecting approach for incompressible Stokes equations*, Internat. J. Numer. Methods Engrg. 94 (2013), pp. 128–149.